Coupled Systems Mechanics, *Vol. 15, No. 3 (2026) 243-262*
https://doi.org/10.12989/csm.2026.15.3.243

Techno-Press

Effect of frequency and nonlocal parameter in nonlocal isotropic thermoelastic diffusive solid due to inclined load

Parveen Lata[1], Belay Fikadu Gerba*[2], Satya Bir Singh[1]

[1]*Department of Mathematics, Punjabi University, Patiala, 147002, India*
[2]*Department of Mathematics, Dambi Dollo University, Oromia, Ethiopia*

(Received February 14, 2026, Revised June 18, 2026, Accepted June 22, 2026)

Abstract. This study investigates the dynamic response of a nonlocal thermoelastic solid with diffusion subjected to an inclined load in the frequency domain. The work aims to analyze the combined influence of nonlocal effects and excitation frequency on the coupled thermoelastic diffusive behavior of the medium, which is important for the accurate modeling of micro- and nano-scale structures. The originality of the study lies in incorporating both nonlocal elasticity and mass diffusion effects under an inclined loading condition within a frequency domain framework. The governing equations are transformed using the time-harmonic approach and Fourier transform technique, leading to analytical expressions for displacement, stress, temperature change, and mass concentration in the transformed domain. Numerical inversion is subsequently employed to obtain the physical-domain solutions. The results reveal that both the nonlocal parameter and angular frequency significantly influence the distributions of mechanical, thermal, and diffusive fields. The presented model provides a useful theoretical framework for understanding coupled thermoelastic diffusive processes in advanced materials and nano-engineered structures.

Keywords: angular frequency; Fourier transformation; inclined load; nonlocal; stress; thermoelasticity

1. Introduction

In nonlocal elasticity theory, the nonlocal parameter characterizes the influence of long-range interatomic interactions and small-scale effects that are not captured by the classical local continuum theory. Physically, it represents the degree to which the stress at a material point depends not only on the strain at that point but also on the strain field in its surrounding neighborhood. As the nonlocal parameter increases, the small-scale effects become more pronounced, leading to a reduction in stiffness and a noticeable modification of the thermoelastic-diffusive response.

[1] established the theory of nonlocal elasticity by introducing constitutive relations in which the stress at a point depends not only on the strain at that point but also on the strains of surrounding particles. This work provided a theoretical framework for modeling size-dependent effects and wave dispersion in materials with microstructural interactions. The theory has since become a fundamental tool in nanomechanics and nonlocal continuum mechanics. [2] further extended nonlocal concepts to thermoelastic materials through the formulation of nonlocal

*Corresponding author, Ph.D., E-mail: Gerbabelay2022@gmail.com

http://www.techno-press.org/csm/5

ISSN: 2234-2184 (Print), 2234-2192 (Online)

thermoelasticity. The proposed theory accounted for long-range interactions in thermoelastic media and provided a framework for studying thermal and mechanical responses in microstructured solids.

[3] developed the linear theory of micropolar elasticity, extending classical elasticity by incorporating rotational degrees of freedom and couple stresses. The theory enabled the analysis of materials with internal microstructures and provided a more realistic description of mechanical behavior at small scales. [4] investigated generalized thermoelastic diffusion interactions under time-harmonic thermal sources. Their study incorporated diffusion effects into thermoelasticity and demonstrated the coupled behavior of thermal, elastic, and mass diffusion fields. [5] studied the disturbance produced by an inclined load in a transversely isotropic thermoelastic medium with two temperatures and without energy dissipation. The investigation emphasized the role of anisotropy and two-temperature effects on the mechanical response of thermoelastic materials.

[6] presented a comprehensive review of continuum theories involving nonlocal elastic responses. They established a general framework for conservative and dissipative systems and discussed various formulations of nonlocal elasticity. [7] investigated thermoelastic diffusion in a thick circular plate within the modified couple stress theory. The study incorporated size-dependent effects and examined the coupled influence of thermal and diffusive fields. [8] considered a thermoelastic diffusion problem in a half-space using a refined dual-phase-lag Green-Naghdi model. The formulation incorporated finite thermal wave speed and diffusion effects, enabling a more realistic representation of thermoelastic processes. [9] investigated the combined effects of nonlocality and two-temperature theory in a nonlocal thermoelastic solid exposed to a ramp-type heat source. The study demonstrated the importance of scale-dependent effects in thermoelastic interactions. [10] studied hyperbolic two-temperature photo-thermal interactions in a semiconductor medium containing a cylindrical cavity. The model incorporated carrier density effects and finite thermal wave propagation, allowing a realistic description of photothermal processes in semiconductors. Their investigation contributed to the growing field of semiconductor thermoelasticity.

[11] employed finite element methods to analyze a nonlinear bioheat model in skin tissue subjected to external thermal sources. The study focused on heat transfer mechanisms in biological tissues and provided numerical predictions of temperature distributions. [12] investigated generalized thermoelastic interactions in a half-space within a nonlocal thermoelastic framework. The study incorporated scale-dependent effects and examined their influence on thermoelastic wave propagation. [13] analyzed axisymmetric deformations in a nonlocal isotropic thermoelastic solid within the framework of two-temperature theory. The work emphasized the combined influence of nonlocality and thermal interactions on stress and displacement fields. Their study contributed to the development of nonlocal thermoelastic plate models.

[14] studied generalized magneto-thermoelastic behavior of layered media within the Lord-Shulman and Green-Lindsay theories. Their work compared different generalized thermoelastic formulations and highlighted the influence of thermal relaxation times. [15] performed finite element analyses of nonlinear dual-phase-lag bioheat models in spherical tissues. Experimental data were incorporated to validate the computational model. The investigation demonstrated the applicability of advanced bioheat theories in biomedical engineering. [16] examined the reflection and transmission of plane waves in nonlocal generalized thermoelastic solids with diffusion. The study explored the interaction between nonlocality, thermoelasticity, and diffusion processes during wave propagation. Their work provided valuable insights into dynamic thermoelastic phenomena. [17] investigated the combined effects of nonlocality and two-temperature theory in

an isotropic thermoelastic thick circular plate without energy dissipation. The analysis focused on thermoelastic interactions under generalized heat conduction assumptions. Their study extended the application of nonlocal thermoelasticity to plate structures.

[18] studied the influence of thermal relaxation times in living tissues using the three-phase-lag bioheat model. The work incorporated experimental considerations and examined thermal responses under biological conditions. [19] analyzed the influence of magnetic fields and inclined loading on a two-dimensional thermoelastic medium under gravity. The study incorporated multiple coupled physical effects within a generalized thermoelastic framework. Their work expanded the applications of magneto-thermoelasticity. [20] investigated thermodiffusion interactions in a homogeneous spherical shell using a modified Moore-Gibson-Thompson model with two time delays. The study combined thermoelastic diffusion theory with advanced heat conduction models. Their formulation provided improved descriptions of thermal wave propagation. [21] examined the structural stability of porous Cosserat media within a generalized continuum framework. The study incorporated porosity and microstructural effects into the stability analysis. [22] developed a fractional Moore-Gibson-Thompson photothermal model for rotating semiconductors. The formulation incorporated fractional derivatives to describe anomalous diffusion and thermal wave propagation. [23] investigated non-simple thermoelastic diffusion interactions in a half-space incorporating both nonlocality and memory effects. The study combined advanced constitutive relations with generalized heat conduction theories. Their work highlighted the importance of hereditary effects in thermoelastic diffusion. [24] examined frequency-domain responses of transversely isotropic thermoelastic diffusive solids with two-temperature effects. The study investigated coupled thermoelastic and diffusion phenomena in anisotropic media. Their work provided useful insights into dynamic thermoelastic diffusion interactions. Several studies have been conducted in this direction recently as [25, 26, 27, 28] and [29].

The effect of nonlocal parameters and the angular frequency are studied by many scholars as we have cited above. More of them worked on area of nonlocal with diffusion of thermoelasticity under a thermal source, heat transfer and mass transport with focus on transient or time-domain analysis. This study focuses on how nonlocal effects and angular frequency influence the stress, temperature change and mass concentration of copper material under inclined mechanical load. There is a critical need for advanced mathematical modeling and analytical techniques to accurately capture these interactions. So we will fill this gap by formulating model, analyze it by using Fourier transformation and MATLAB software and it will ultimately improving their practical applications.

2. Basic equations

Following [30] the stress tensor at arbitrary point x of a nano material body not only depends up on the stress tensor at x, but also depend on all points of the body. The nonlocal stress tensor σij for a homogeneous isotropic elastic material can be expressed as

$$\sigma_{ij}(x) = \int_V \alpha(|x - x'|, \xi)\, t_{ij}(x) dV(x')\,, \tag{1}$$

By employing Eringen's nonlocal formulation, the nonlocal stress tensor σij(x) can be expressed as

$$(1 - \xi^2\nabla^2)\sigma_{ij}(x) = t_{ij}(x), \tag{2}$$

The constitutive equation for coupled thermoelastic diffusion medium while neglecting the body forces can be expressed as

$$\begin{gathered}(1 - \xi^2\nabla^2)\sigma_{ij}(x) = 2\mu e_{ij}(x) + \delta_{ij}(\lambda e_{kk} - \gamma_1 T - \gamma_2 C),\\ P = -\gamma_2\, e_{kk} - aT + bC.\end{gathered} \tag{3}$$

Following [2, 16, 31] the basic equations in isotropic nonlocal thermoelastic media with diffusion can be given by

$$(\lambda + \mu)\nabla\cdot\nabla u + \mu\nabla^2 u - \gamma_1\nabla T - \gamma_2\nabla C + \rho(1 - \xi^2\nabla^2)F = \rho(1 - \xi^2\nabla^2)\ddot{u}, \tag{4}$$

$$\left(K\frac{\partial}{\partial t} + K^*\right)\nabla^2 T = \rho(1 - \xi^2\nabla^2)\frac{\partial^2}{\partial t^2}(\rho C_e T + \gamma_1 T_0 u_{i,i} + aT_0 C), \tag{5}$$

$$(1 - \xi^2\nabla^2)\dot{C} = d\nabla^2(bC - \gamma_2 e_{kk} - aT). \tag{6}$$

where

$$\gamma_1 = (3\lambda + 2\mu)\alpha_t, \quad \gamma_2 = (3\lambda + 2\mu)\alpha_c. \tag{7}$$

T =temperature change, ρ =density, α_t =coefficient of thermal expansion,
α_c =coefficient of diffusion, K =coefficient of thermal conductivity,
K^* =materialistic constant, a =coefficient of thermoelastic diffusive effects,
b =coefficient of diffusive effects, σ_{ij} =components of the stress tensor,
C =mass concentration, u_i=displacement vector, λ and μ =Lamé's constants,
C_e =specific heat at constant strain, T_0 =temperature of the medium in its natural state,
d=diffusion constant, ξ=nonlocal parameter, $e_{ij} = ½(u_{i,j} + u_{j,i})$, i, j=1, 2, 3,
∇=gradient operator, ∇^2 =Laplacian operator.

3. Formulation and solution of the problem

Considering a two dimensional homogeneous nonlocal isotropic thermoelastic body initialy at undeformed state at initial temperature T_0. We take a rectangular coordinate system (x,y,z) having origin on the surface z=0 with z-axis pointing vertically downward into the medium is introduced. The analysis will be carried in frequency domain. The surface of half space is subjected to inclined load. Inclined load is a linear combination of tangential load and normal load. For two dimensional problem in xz plane we take

$$\boldsymbol{u} = (u, 0, w), u = u(x,z,t),\ w = w(x,z,t),\ T = T(x,z,t) \text{ and } C = C(x,z,t). \tag{8}$$

Using (8) in Eqs. (4)-(6), the corresponding formulation in xz-plane reduces to

$$(\lambda + \mu)\frac{\partial e}{\partial x} + \mu\nabla^2 u - \gamma_1\frac{\partial T}{\partial x} - \gamma_2\frac{\partial C}{\partial x} + \rho(1 - \xi^2\nabla^2)F_1 = \rho(1 - \xi^2\nabla^2)\ddot{u}, \tag{9}$$

$$(\lambda + \mu)\frac{\partial e}{\partial z} + \mu\nabla^2 w - \gamma_1\frac{\partial T}{\partial z} - \gamma_2\frac{\partial C}{\partial z} + \rho(1 - \xi^2\nabla^2)F_3 = \rho(1 - \xi^2\nabla^2)\ddot{w}, \tag{10}$$

$$\left(K\frac{\partial}{\partial t} + K^*\right)\nabla^2 T = \rho(1 - \xi^2\nabla^2)\frac{\partial^2}{\partial t^2}(\rho C_E T + \gamma^1 T^0 e + aT^0 C), \tag{11}$$

$$(1-\xi^2\nabla^2)\frac{\partial C}{\partial t}=d\left(b\left(\frac{\partial^2 C}{\partial x^2}+\frac{\partial^2 C}{\partial z^2}\right)-\gamma_2\left(\frac{\partial^2}{\partial x^2}+\frac{\partial^2}{\partial z^2}\right)\left(\frac{\partial u}{\partial x}+\frac{\partial w}{\partial z}\right)-a\left(\frac{\partial^2 T}{\partial x^2}+\frac{\partial^2 T}{\partial z^2}\right)\right) \tag{12}$$

The initial and regularity conditions of the above problems are given by

$$\begin{gathered} u(x,z,0)=0=\dot{u}(x,z,0) \\ w(x,z,0)=0=\dot{w}(x,z,0) \\ T(x,z,0)=0=\dot{T}(x,z,0) \\ C(x,z,0)=0=\dot{C}(x,z,0), for\ z\geq 0,-\infty<x<\infty \\ u(x,z,t)=w(x,z,t)=T(x,z,t)=C(x,z,t)=0, for\ t>0, when\ z\to\infty \end{gathered} \tag{13}$$

We use dimensionless quantities to simplify the solution as

$$\begin{gathered} x'=\frac{\omega_1^*}{c_1}x,\quad z'=\frac{\omega_1^*}{c_1}z,\quad t'=\omega_1^*\mathrm{t},\quad \mathrm{u}'=\frac{\omega_1^*}{c_1}u,\quad a'=\frac{\omega_1^*}{c_1}a, \\ w'=\frac{\omega_1^*}{c_1}w,\quad C'=\frac{\gamma_2 C}{\rho {c_1}^2},\quad T'=\frac{\gamma_1 T}{\rho {c_1}^2},\quad {F_1}'=\frac{F_1}{\gamma_1 T_0} \\ F^{3\prime}=\frac{F^3}{\gamma^1 T^0},\quad e'=e, {c_1}^2=\frac{(\lambda+2\mu)}{\rho}\quad \omega_1^*=\frac{\rho C_E {c_1}^2}{K} \end{gathered} \tag{14}$$

For the decoupling of equations, express $u(x,z,t)$ and $w(x,z,t)$ by dimensionless potential functions Ψ_1 and Ψ_2 as follows

$$u=\frac{\partial\Psi_1}{\partial x}-\frac{\partial\Psi_2}{\partial z}\qquad w=\frac{\partial\Psi_1}{\partial z}+\frac{\partial\Psi_2}{\partial x}, \tag{15}$$

We consider the time harmonic behavior given by

$$(\mathrm{u},\mathrm{w},\mathrm{T},\mathrm{C})(\mathrm{x},\mathrm{z},\mathrm{t})=(\mathrm{u},\mathrm{w},\mathrm{T},\mathrm{C})(\mathrm{x},\mathrm{z})\mathrm{e}^{\mathrm{i}\omega\mathrm{t}}, \tag{16}$$

The Fourier transformation is given as follow

$$\mathrm{f}(\zeta,\mathrm{z},\mathrm{t})=\int_{-\infty}^{\infty}\mathrm{f}(\mathrm{x},\mathrm{z},\mathrm{t})\,\mathrm{e}^{(-\mathrm{i}\zeta\mathrm{x})}\mathrm{dx}. \tag{17}$$

By using dimensionless quantities defined by (14) in Eqs. (9)-(12) and suppressing the primes from them, then substitute Eq. (15) in them and applying Eqs. (16)-(17) on resulting equations, yields

$$\left(\mathrm{A}_1(\mathrm{D}^2-\zeta^2)+\omega^2\left(1-\mathrm{A}_{11}(\mathrm{D}^2-\zeta^2)\right)\right)\widehat{\Psi}_1-\widehat{T}-\hat{\mathrm{C}}=0, \tag{18}$$

$$\left(A_2(D^2-\zeta^2)+\left(1-A_{11}(D^2-\zeta^2)\right)\omega^2\right)\widehat{\Psi}_2=0, \tag{19}$$

$$\begin{gathered} A_3\left(1-A_{11}(D^2-\zeta^2)\right)(D^2-\zeta^2)\widehat{\Psi}_1+\left(A^4\left(1-A_{11}(D^2-\zeta^2)\right)-A_5(D^2-\zeta^2)\right)\widehat{T}+ \\ A_6(1-A_{11}(D^2-\zeta^2))\hat{\mathrm{C}}=0, \end{gathered} \tag{20}$$

$$\begin{gathered} A_9(D^2-\zeta^2)^2\widehat{\Psi}_1+A_{10}(D^2-\zeta^2)\widehat{T}+[A_7(1-A_{11}(D^2-\zeta^2))- \\ A_8(D^2-\zeta^2)]\hat{\mathrm{C}}=0. \end{gathered} \tag{21}$$

where:

$$A_1=\frac{\lambda+2\mu}{\rho {c_1}^2},\quad A_2=\frac{\mu}{\rho {c_1}^2},\quad A_3=\rho-\omega^2\gamma_1 T_0,\quad A_4=-i\omega^3\left(\frac{\rho^3 {c_1}^2 {\omega_1}^*}{\gamma^1}\right)C_E,$$

$$A_5 = \left(\frac{\rho c_1}{\gamma_1}\right)(K\omega_1{}^*\mathrm{i}\omega + K^*),\ A_6 = -\omega^2\left(\frac{\rho^2 c_1{}^3}{\omega_1{}^*\gamma_2}\right)T_0 a',\quad A_7 = \left(\frac{\rho\omega_1{}^* c_1{}^2}{\gamma_2}\right)i\omega,$$
$$A_8 = db\left(\frac{\rho\omega_1{}^*}{\gamma^2}\right),\ A_9 = d\gamma^2\left(\frac{\omega}{c^{12}}\right),\ A_{10} = ad\left(\frac{\rho\omega_1{}^{*2}}{\gamma_1}\right),\ A_{11} = \frac{\omega_1{}^{*2}\xi^2}{c_1{}^2},\ A_{12} = \gamma_1 T_0,$$
$$A_{13} = \frac{\rho\omega_1{}^* c_1}{\gamma_1},\quad A_{14} = \gamma_1 T_0,\quad A_{15} = \frac{\rho\omega_1{}^* c_1}{\gamma_2},\ A_{16} = \frac{A_{12}}{A_{13}},\ A_{17} = \frac{A_{14}}{A_{13}}.$$

The Eqs. (18)-(21) possess a nontrivial solution if determinant of their coefficients vanishes, which yields

$$(D^6 R_1 + D^4 R_2 + D^2 R_3 + R_4)(\widehat{\Psi}_1, \hat{T}, \hat{C}) = 0. \tag{22}$$

$$(D^2 + r)\widehat{\Psi}_2 = 0,\qquad r = \frac{R_6}{R_5}. \tag{23}$$

where:

$$M_1 = -A_4A_7\omega^2, M_2 = A_1A_4A_7 + A_4A_8\omega^2 - A_5A_7\omega^2 - A_6A_{10}\omega^2 + A_3A_7,$$
$$M_3 = -A_1A_4A_8 + A_5A_8\omega^2,\quad M_4 = A_1A_5A_7 + A_1A_6A_{10} + A_3A_8 + A_9A_6 + A_3A_{10} - A_4A_9,$$
$$M_5 = A_1A_5A_8 - A_5A_9,\ M_6 = M_2A_{11}{}^2 - A_{11}{}^3M_1 + M_4A_{11} + M_5,$$
$$M_7 = A_{11}{}^2M_1 - 2M_2A_{11} - M_3A_{11} - M_4,\ M_8 = M_2 + M_3 - 3A_{11}M_1,\ M_9 = M_1,$$
$$R_1 = M_6,\ R_2 = -3M_6\zeta^2 + M_7,\ R_3 = 3M_6\zeta^4 - 2M_7\zeta^2 + M_8,$$
$$R_4 = M_7\zeta^4 + M_9 - M_6\zeta^6 - M_8\zeta^2,\ R_5 = A_2 - A_{11}\omega^2,$$
$$R_6 = -A_{11}\zeta^2\omega^2 - A_2\zeta^2 - 1.$$

When we solve Eq. (22) we get their roots $\pm r_i$, (i=1, 2, 3) and roots are $\pm r_4$ of the equation (23). Also the solution vanishes as z→∞, therefore general solution is given in the following form.

$$\widehat{\Psi_1} = B_1e^{-r_1z} + B_2e^{-r_2z} + B_3e^{-r_3z}, \tag{24}$$

$$\hat{T} = d_1B_1e^{-r_1z} + d_2B_2e^{-r_2z} + d_3B_3e^{-r_3z}, \tag{25}$$

$$\hat{C} = l_1B_1e^{-r_1z} + l_2B_2e^{-r_2z} + l_3B_3e^{-r_3z}, \tag{26}$$

$$\widehat{\Psi}_2 = B_4e^{-r_4z}. \tag{27}$$

where d_i and l_i are given by

$$d_{\mathrm{i}} = \frac{(r_{\mathrm{i}}{}^6M_{13} + r_{\mathrm{i}}{}^4M_{14} + r_{\mathrm{i}}{}^2M_{15} + M_{16})}{(r_{\mathrm{i}}{}^4M_{10} + r_{\mathrm{i}}{}^2M_{11} + M_{12})},\qquad i = (1,2,3)$$
$$l_{\mathrm{i}} = \frac{(r_{\mathrm{i}}{}^6M_{17} + r_{\mathrm{i}}{}^4M_{18} + r_{\mathrm{i}}{}^2M_{19} + M_{20})}{(r_{\mathrm{i}}{}^4M_{10} + r_{\mathrm{i}}{}^2M_{11} + M_{12})}.\qquad i = (1,2,3)$$

where:

$$N_1 = A_1 - \omega^2A_{11},\ N_2 = (A_1 - \omega^2A_{11})\zeta^2 + \omega^2,\ N_3 = -A_3A_{11},\ N_4 = A_3 + 2A_3A_{11}\zeta^2,$$
$$N_5 = -A_3A_{11}\zeta^4 + A_3\zeta^2,\ N_6 = -A_4A_{11} - A_5,\ N_7 = A_4 + A_4A_{11}\zeta^2 + A_5\zeta^2,\ N_8 = A_6A_{11},$$
$$N_9 = A_6A_{11}\zeta^2 + A_6,\ N_{10} = A_9,\ N_{11} = 2A_9\zeta^2,\ N_{12} = A_9\zeta^4,\ N_{13} = A_{10},\ N_{14} = A_{10}\zeta^2,$$
$$N_{15} = -A_7A_{11} - A_8,\ N_{16} = (A_7A_{11} + A_8)\zeta^2 + A_7,\ N_{17} = A_2 + \omega^2A_{11},\ N_{18} = (A_2 - \omega^2A_{11})\zeta^2 + \omega^2,\ M_{10} = N_6N_{15} + N_8N_{13},\ M_{11} = N_6N_{16} + N_7N_{15} - N_9N_{13} - N_8N_{14},$$
$$M_{12} = N_7N_{16} + N_9N_{14},\ M_{13} = -N_3N_{15} - N_8N_{10},\ M_{14} = N_9N_{10} - N_3N_6 - N_4N_{15} + N_9N_{10} + N_8N_{11},\ M_{15} = N_4N_{16} - N_5N_{15} - N_9N_{11} - N_8N_{12},\ M_{16} = N_5N_{16} + N_9N_{12},$$
$$M_{17} = -N_3N_{13} - N_6N_{10},\ M_{18} = N_6N_{11} - N_7N_{10} + N_4N_{13} - N_3N_{14},\ M_{19} = N_7N_{11} - N_6N_{12} - N_5N_{13} - N_4N_{14},\ M_{20} = N_5N_{14} - N_7N_{12}.$$

4. Boundary conditions

On the half-space $z = 0$ mechanical forces are applied. We consider the appropriate boundary condition as

$$(1 - \xi^2\nabla^2)\sigma_{zz} = -F_1\varphi_1(x)e^{i\omega t}, \tag{28}$$

$$(1 - \xi^2\nabla^2)\sigma_{zx} = -F_2\varphi_2(x)e^{i\omega t}, \tag{29}$$

$$\frac{\partial T\ (x,z,t)}{\partial z} = 0, \tag{30}$$

$$\frac{\partial C(x,z,t)}{\partial z} = 0. \tag{31}$$

where: F_1, F_2 are mechanical force applied and $\varphi_1(x)$ and $\varphi_2(x)$ specify the horizontal and vertical load distribution functions, ω is angular frequency.

By applying Fourier transformation given by Eq. (17) on the equations Eqs. (28)-(31) after simplification we get

$$M_{21}B_1 + M_{22}B_2 + M_{23}B_3 + M_{24}B_4 = -F_1\hat{\varphi}_1(\zeta)e^{i\omega t}, \tag{32}$$

$$M_{25}B_1 + M_{26}B_2 + M_{27}B_3 + M_{28}B_4 = -F_2\hat{\varphi}_2(\zeta)e^{i\omega t}, \tag{33}$$

$$M_{29}B_1 + M_{30}B_2 + M_{31}B_3 = 0, \tag{34}$$

$$M_{32}B_1 + M_{33}B_2 + M_{34}B_3 = 0. \tag{35}$$

where:

$$M_{21} = A_{11}\lambda({r_1}^2 - \zeta^2) - \lambda {A_{11}}^2({r_1}^4 - 2\zeta^2{r_1}^2 + \zeta^4) - 2\mu r_1 + 2\mu A_{11}{r_1}^3 - 2\mu A_{11}\zeta^2 r_1 - A_3 d_1 - A_{11}A_3 d_1{r_1}^2 + A_{11}A_3\zeta^2 d_1 - A_3 l_1 - A_{11}A_3 l_1 {r_1}^2 + A_{11}A_3\zeta^2 l_1,$$

$$M_{22} = A_{11}\lambda({r_2}^2 - \zeta^2) - \lambda {A_{11}}^2({r_2}^4 - 2\zeta^2{r_2}^2 + \zeta^4) - 2\mu r_2 + 2\mu A_{11}{r_2}^3 - 2\mu A_{11}\zeta^2 r_2 - A_3 d_2 - A_{11}A_3 d_2{r_2}^2 + A_{11}A_3\zeta^2 d_2 - A_3 l_2 - A_{11}A_3 l_2 {r_2}^2 + A_{11}A_3\zeta^2 l_2,$$

$$M_{23} = A_{11}\lambda({r_3}^2 - \zeta^2) - \lambda {A_{11}}^2({r_3}^4 - 2\zeta^2{r_3}^2 + \zeta^4) - 2\mu r_3 + 2\mu A_{11}{r_3}^3 - 2\mu A_{11}\zeta^2 r_3 - A_3 d_3 - A_{11}A_3 d_3{r_3}^2 + A_{11}A_3\zeta^2 d_3 - A_3 l_3 - A_{11}A_3 l_3 {r_3}^2 + A_{11}A_3\zeta^2 l_3,$$

$$M_{24} = i\zeta - A_{11}i\zeta {r_4}^2 + A_{11}i\zeta^3,\ M_{25} = \mu[-r_1 + A_{11}({r_1}^3 - \zeta^2 r_1)],$$

$$M_{26} = \mu[-r_2 + A_{11}({r_2}^3 - \zeta^2 r_2)], \quad M_{27} = \mu[-r_3 + A_{11}({r_3}^3 - \zeta^2 r_3)],$$

$$M_{28} = \mu[i\zeta - A_{11}(i\zeta {r_4}^2 - i\zeta^3)], \quad M_{29} = -r_1 d_1, \quad M_{30} = -r_2 d_2, \quad M_{31} = -r_3 d_3,$$

$$M_{32} = r_1 l_1, \quad M_{33} = r_2 l_2, \quad M_{34} = r_3 l_3.$$

when we solve the system of Eqs. (32)-(35), we get the nontrivial values of $B_i, i = 1, 2, 3, 4$ given by

$$B_1 = -\frac{F_1\hat{\varphi}_1(\zeta)}{\Delta s}\Delta_1 + \frac{F_2\hat{\varphi}_2(\zeta)}{\Delta s}\Delta_2, \tag{36}$$

$$B_2 = \frac{F_1\hat{\varphi}_1(\zeta)}{\Delta s}\Delta_3 - \frac{F_2\hat{\varphi}_2(\zeta)}{\Delta s}\Delta_4, \tag{37}$$

$$B_3 = -\frac{F_1\hat{\varphi}_1(\zeta)}{\Delta s}\Delta_5 + \frac{F_2\hat{\varphi}_2(\zeta)}{\Delta s}\Delta_6, \tag{38}$$

$$B_4 = \frac{F_1\hat{\varphi}_1(\zeta)}{\Delta s}\Delta_7 - \frac{F_2\hat{\varphi}_2(\zeta)}{\Delta s}\Delta_8. \tag{39}$$

where:

$$\Delta = \mathrm{M}_{24}\mathrm{M}_{27}\mathrm{M}_{30}\mathrm{M}_{32} - \mathrm{M}_{23}\mathrm{M}_{28}\mathrm{M}_{30}\mathrm{M}_{32} - \mathrm{M}_{24}\mathrm{M}_{26}\mathrm{M}_{31}\mathrm{M}_{32} + \mathrm{M}_{22}\mathrm{M}_{28}\mathrm{M}_{31}\mathrm{M}_{32} - \mathrm{M}_{24}\mathrm{M}_{27}\mathrm{M}_{29}\mathrm{M}_{33} + \mathrm{M}_{23}\mathrm{M}_{28}\mathrm{M}_{29}\mathrm{M}_{33} + \mathrm{M}_{24}\mathrm{M}_{25}\mathrm{M}_{31}\mathrm{M}_{33} - \mathrm{M}_{21}\mathrm{M}_{28}\mathrm{M}_{31}\mathrm{M}_{33} + \mathrm{M}_{24}\mathrm{M}_{26}\mathrm{M}_{29}\mathrm{M}_{34} - \mathrm{M}_{22}\mathrm{M}_{28}\mathrm{M}_{29}\mathrm{M}_{34} - \mathrm{M}_{24}\mathrm{M}_{25}\mathrm{M}_{30}\mathrm{M}_{34} + \mathrm{M}_{21}\mathrm{M}_{28}\mathrm{M}_{30}\mathrm{M}_{34},$$

$$\Delta_1 = \mathrm{M}_{28}(\mathrm{M}_{30}\mathrm{M}_{34} - \mathrm{M}_{31}\mathrm{M}_{33}),\ \ \Delta_2 = \mathrm{M}_{24}(\mathrm{M}_{30}\mathrm{M}_{34} - \mathrm{M}_{31}\mathrm{M}_{33}),$$

$$\Delta_3 = \mathrm{M}_{28}(\mathrm{M}_{29}\mathrm{M}_{34} - \mathrm{M}_{31}\mathrm{M}_{32}),\ \ \Delta_4 = \mathrm{M}_{24}(\mathrm{M}_{29}\mathrm{M}_{34} - \mathrm{M}_{31}\mathrm{M}_{32}),$$

$$\Delta_5 = \mathrm{M}_{28}(\mathrm{M}_{29}\mathrm{M}_{33} - \mathrm{M}_{30}\mathrm{M}_{32}),\ \ \Delta_6 = \mathrm{M}_{24}(\mathrm{M}_{29}\mathrm{M}_{33} - \mathrm{M}_{30}\mathrm{M}_{32}),$$

$$\Delta_7 = \mathrm{M}_{25}(\mathrm{M}_{30}\mathrm{M}_{34} - \mathrm{M}_{31}\mathrm{M}_{33}) - \mathrm{M}_{26}(\mathrm{M}_{29}\mathrm{M}_{34} - \mathrm{M}_{31}\mathrm{M}_{32}) + \mathrm{M}_{27}(\mathrm{M}_{29}\mathrm{M}_{33} - \mathrm{M}_{30}\mathrm{M}_{32}),$$

$$\Delta_8 = \mathrm{M}_{21}(\mathrm{M}_{30}\mathrm{M}_{34} - \mathrm{M}_{31}\mathrm{M}_{33}) - \mathrm{M}_{22}(\mathrm{M}_{29}\mathrm{M}_{34} - \mathrm{M}_{31}\mathrm{M}_{32}) + \mathrm{M}_{23}(\mathrm{M}_{29}\mathrm{M}_{33} - \mathrm{M}_{30}\mathrm{M}_{32}).$$

By applying Fourier transform on Eq. (15), substitute from Eq. (24)-(27), using Eqs. (36)-(39) we get expressions for components of displacement, stress, temperature change and mass concentration as given by

$$\hat{\mathrm{u}} = -\left(\frac{F_1\hat{\varphi}_1(\zeta)}{\Delta}\Delta_{11} + \frac{F_2\hat{\varphi}_2(\zeta)}{\Delta}\Delta_{12}\right)e^{i\omega t} \tag{40}$$

$$\hat{\mathrm{w}} = \left(\frac{F_1\hat{\varphi}_1(\zeta)}{\Delta}\Delta_{13} - \frac{F_2\hat{\varphi}_2(\zeta)}{\Delta}\Delta_{14}\right)e^{i\omega t} \tag{41}$$

$$\hat{T} = \left(-\frac{F_1\hat{\varphi}_1(\zeta)}{\Delta}\Delta_{15} + \frac{F_2\hat{\varphi}_2(\zeta)}{\Delta}\Delta_{16}\right)e^{i\omega t} \tag{42}$$

$$\hat{\mathrm{C}} = \left(-\frac{F_1\hat{\varphi}_1(\zeta)}{\Delta}\Delta_{17} + \frac{F_2\hat{\varphi}_2(\zeta)}{\Delta}\Delta_{18}\right)e^{i\omega t} \tag{43}$$

$$\hat{\sigma}_{zz} = \left(\frac{F_1\hat{\varphi}_1(\zeta)}{\Delta}\Delta_{19} + \frac{F_2\hat{\varphi}_2(\zeta)}{\Delta}\Delta_{20}\right)e^{i\omega t} \tag{44}$$

$$\hat{\sigma}_{zx} = \left(-\frac{F_1\hat{\varphi}_1(\zeta)}{\Delta}\Delta_{21} - \frac{F_2\hat{\varphi}_2(\zeta)}{\Delta}\Delta_{22}\right)e^{i\omega t} \tag{45}$$

Where

$$\Delta_{11} = i\zeta\Delta_1 e^{-\mathrm{r1z}} - i\zeta\Delta_3 e^{-\mathrm{r2z}} + i\zeta\Delta_5 e^{-\mathrm{r3z}} + r_4\Delta_7 e^{-\mathrm{r4z}},\quad \Delta_{12} = i\zeta\Delta_2 e^{-\mathrm{r1z}} - i\zeta\Delta_4 e^{-\mathrm{r2z}} + i\zeta\Delta_6 e^{-\mathrm{r3z}} + r_4\Delta_8 e^{-\mathrm{r4z}},\quad \Delta_{13} = \Delta_1 r_1 e^{-\mathrm{r1z}} - \Delta_3 r_2 e^{-\mathrm{r2z}} + \Delta_5 r_3 e^{-\mathrm{r3z}} - i\zeta\Delta_7 e^{-\mathrm{r4z}}\Delta_{14} = \Delta_2 r_1 e^{-\mathrm{r1z}} - \Delta_4 r_2 e^{-\mathrm{r2z}} + \Delta_6 r_3 e^{-\mathrm{r3z}} - i\zeta\Delta_8 e^{-\mathrm{r4z}},\quad \Delta_{15} = \Delta_1 d_1 e^{-\mathrm{r1z}} - \Delta_3 d_2 e^{-\mathrm{r2z}} + \Delta_5 d_3 e^{-\mathrm{r3z}}\Delta_{16} = \Delta_2 d_1 e^{-\mathrm{r1z}} - \Delta_4 d_2 e^{-\mathrm{r2z}} + \Delta_6 d_3 e^{-\mathrm{r3z}},\ \Delta_{17} = \Delta_1 l_1 e^{-\mathrm{r1z}} - \Delta_3 l_2 e^{-\mathrm{r2z}} + \Delta_5 l_3 e^{-\mathrm{r3z}}\Delta_{18} = \Delta_2 l_1 e^{-\mathrm{r1z}} - \Delta_4 l_2 e^{-\mathrm{r2z}} + \Delta_6 l_3 e^{-\mathrm{r3z}},\ \Delta_{19} = G_1\Delta_1 e^{-\mathrm{r1z}} + G_2\Delta_3 e^{-\mathrm{r2z}} - G_3\Delta_5 e^{-\mathrm{r3z}} + G_4\Delta_7 e^{-\mathrm{r4z}},\ \Delta_{20} = G_1\Delta_2 e^{-\mathrm{r1z}} - G_2\Delta_4 e^{-\mathrm{r2z}} + G_3\Delta_6 e^{-\mathrm{r3z}} - G_4\Delta_8 e^{-\mathrm{r4z}}\Delta_{21} = H_1\Delta_1 e^{-\mathrm{r1z}} + H_2\Delta_3 e^{-\mathrm{r2z}} + H_3\Delta_5 e^{-\mathrm{r3z}} + ({r_4}^2 - \zeta^2)\Delta_7 e^{-\mathrm{r4z}},$$

$$\Delta_{22} = H_1\Delta_2 e^{-\mathrm{r1z}} - H_2\Delta_4 e^{-\mathrm{r2z}} + H_3\Delta_6 e^{-\mathrm{r3z}} - ({r_4}^2 - \zeta^2)\Delta_8 e^{-\mathrm{r4z}}\ \ , G_\mathrm{i} = (\lambda + 2\mu){r_\mathrm{i}}^2 + \lambda\zeta^2 - \frac{\rho {c_1}^2 d_\mathrm{i}}{C} - \frac{\rho {c_1}^2 l_\mathrm{i}}{C},\ \ H_\mathrm{i} = -2r_\mathrm{i} i\zeta\mu,$$

5. Specific loads

5.1 Concentrated force

The disturbance on half space due to concentrated normal force is solved by setting the following relation

$$\varphi_1(x) = \varphi_2(x) = \delta(x)\ , \tag{46}$$

Where $\delta()$ is Dirac delta function and after applying Fourier transformation on it we get

$$\hat{\varphi}_1(\zeta) = \hat{\varphi}_2(\zeta) = 1. \tag{47}$$

5.2 Uniformly distributed force

In this case we consider

$$\{\varphi_1(x), \varphi_2(x)\} = \begin{cases} 1, if\ |x| \le m \\ 0, if\ |x| > m \end{cases} \tag{48}$$

When we apply the Fourier transformation on Eq. (48) we get the following for the case of uniformly strip load of non-dimensional width 2 m applied at origin.

$$\{\hat{\varphi}_1(\zeta),\ \hat{\varphi}_2(\zeta)\} = \left[2\frac{sin(\zeta m)}{\zeta}\right], \quad \zeta \ne 0 \tag{49}$$

5.3 Linearly distributed force

The solution due to linearly applied force applied on half space is obtained by setting

$$\{\varphi_1(x), \varphi_2(x)\} = \begin{cases} 1 - \frac{|x|}{m}, if\ |x| \le m \\ \quad 0,\ if\ |x| > m \end{cases} \tag{50}$$

By using the Fourier transformation on Eq. (50), that linearly distributed on 2 m width of the strip load, we get

$$\{\hat{\varphi}_1(\zeta),\ \hat{\varphi}_2(\zeta)\} = \frac{2(1 - \cos(\zeta m))}{m\zeta^2}, \quad \zeta \ne 0 \tag{51}$$

Using Eqs. (47), (49), and (51) in Eqs. (40)-(45), we obtain components of displacements, temperature change and mass concentration and stresses due to concentrated load, uniformly distributed load and linearly distributed load respectively.

6. Applications

Suppose an inclined load, per unit length F, is acting on the y-axis and its inclination with z-axis is θ.

From the above graph the horizontal component F_1 and vertical component F_2 of forces are given as

$$\mathrm{F}_1 = \mathrm{F}\cos(\theta), \mathrm{F}_2 = \mathrm{F}\sin(\theta) \tag{52}$$

Using Eq. (52) in Eqs. (40)-(45) we obtain the mathematical expressions of the displacement,

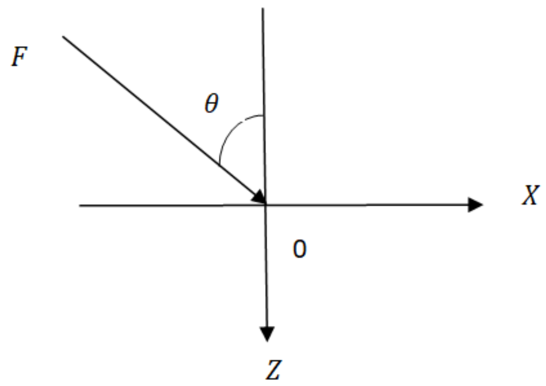

Figure 1. Inclined force applied at the origin of nonlocal isotropic thermoelastic solid

temperature change and mass concentration of nonlocal thermoelastic solid under inclined load based on different angles of inclination.

7. Inversion of Fourier transformations

In order to get the solution of given problem in the physical domain, the inverse of Fourier transform has been employed as suggested by [24].

$$f(x,z,\omega) = \frac{1}{2\pi}\int_{-\infty}^{\infty} e^{-i\zeta x}\hat{f}(\zeta,z,\omega)d(\zeta) = \frac{1}{\pi}\int_{0}^{\infty} |cos(\zeta x)f_{\mathrm{i}} - sin(\zeta x)f_{\mathrm{ii}}|\, d\zeta \tag{58}$$

Where f_{i} and f_{ii} are respectively the odd and even parts of the function $f(\zeta,z,\omega)$.

8. Particular cases

1. When we use $b = 0$ in Eqs. (9)-(12), we get from Eqs. (44)-(49) results for displacement components, temperature change, mass concentration and stress components without diffusion in nonlocal isotropic thermoelastic media.
2. If we take $\xi = 0$, we derive from Eqs. (44)-(49) the displacement components, temperature change, mass concentration and stress components of isotropic thermoelastic solid.

9. Numerical results and discussion

We consider the copper material. As mentioned in the studies of [16], the material constants of copper metal are given by the following table.

In the Figs. 2-6 below

I. Red dashed line is corresponds to $\omega = 1$ and $\xi = 0, 12$

II. Blue line with star is corresponds to $\omega = 0.5$ and $\xi = 0$.

III. Purple line is corresponds to $\omega = 1$ and $\xi = 0.02$.

IV. Black line with triangle marker (>) corresponds to $\omega = 0.5$ and $\xi = 0.02$.

Table 1. Copper material constants

Quantity	Value	Unit
λ	7.76×10^{10}	Nm^{-2}
μ	3.86×10^{10}	Nm^{-2}
α_t	1.78×10^{-5}	K^{-1}
ρ	8954	kgm^{-3}
γ_1	0.02	S
γ_2	0.2	S
K	386	$Wm^{-1}K^{-1}$
A	1.2×10^{4}	$m^2K^{-1}s^2$
B	9×10^{5}	$kgm^{-1}s^{-2}$
T_0	293	K
C_e	383.1	$Jkg^{-1}K^{-1}$
D	8.5×10^{-9}	M
K*	1.2	WmK^{-1}

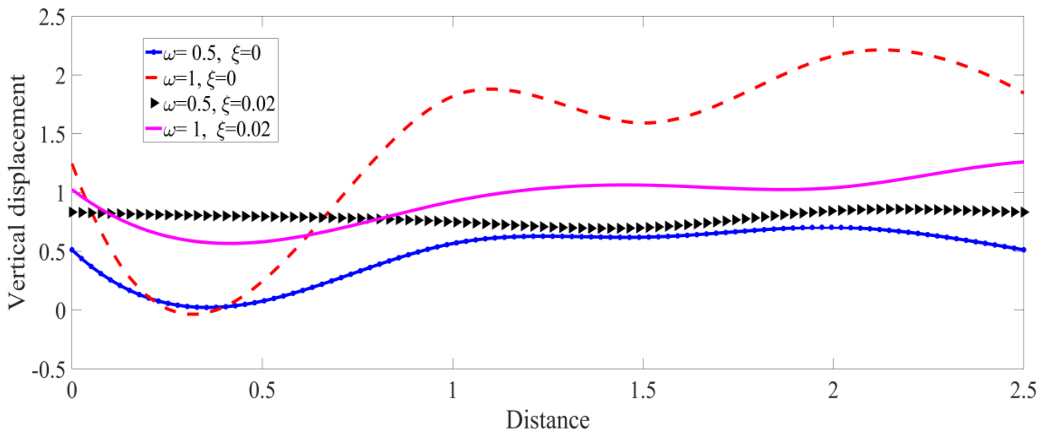

Figure 2. Variation in vertical displacement with distance *x* due to concentrated force

The values of the nonlocal parameter employed in the numerical analysis are selected from the range commonly adopted in the literature on nonlocal thermoelasticity and nanostructures. These values satisfy the requirement that the nonlocal effects remain significant while preserving the physical stability of the model. Furthermore, the chosen range enables a clear comparison between the local case (nonlocal parameter approaching zero) and the nonlocal case, thereby illustrating the sensitivity of displacement, stress, temperature, and concentration fields to small-scale effects.

The Figs. 2-6 represent the graphs of vertical displacement, temperature change, mass concentration, normal stress, and shear stress under an applied inclined load at different angular frequencies and nonlocal parameters.

Fig. 2 shows that the vertical displacement varies along the distance in an oscillatory manner due to the action of the inclined force. It is observed that a higher frequency ($\omega = 1$) produces larger displacement amplitudes compared to the lower frequency ($\omega = 0.5$). The inclusion of the nonlocal parameter ($\xi = 0.02$) reduces and smoothens the displacement response, indicating that

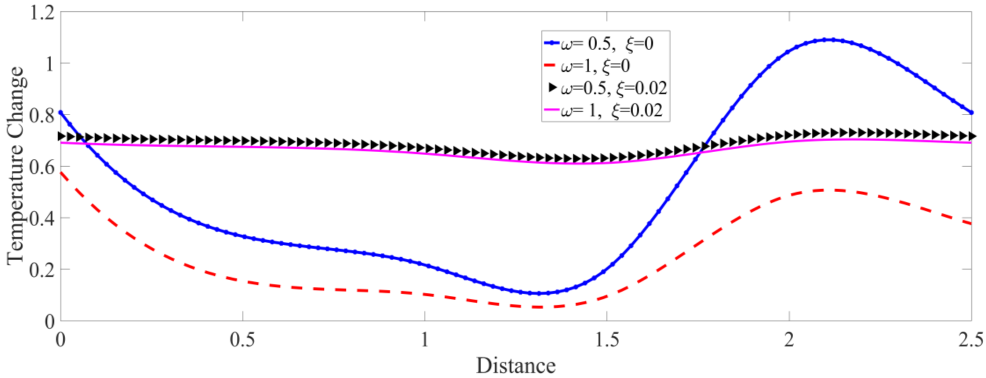

Figure 3. Variation in temperature change with distance *x* due to concentrated force

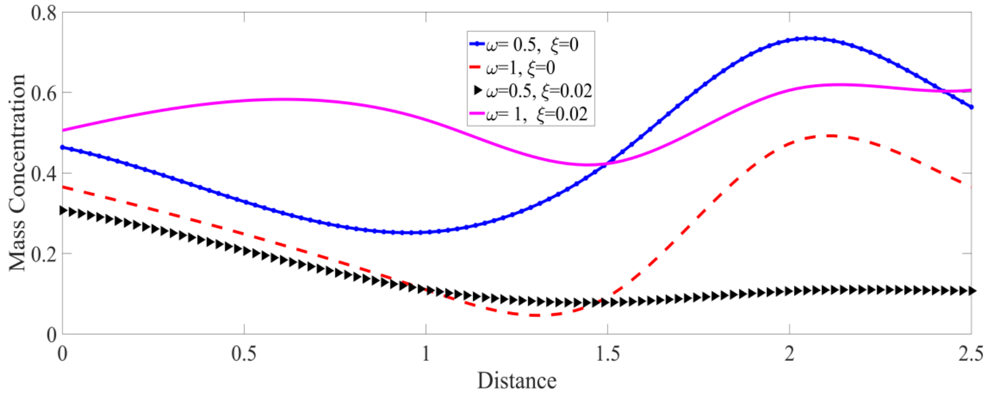

Figure 4. Variation in mass concentration with distance *x* due to concentrated force

nonlocal effects weaken the mechanical deformation and make the response more stable.

Fig. 3 indicates that the temperature change decreases initially with distance, reaches a minimum, and then increases, exhibiting wave-like thermal behavior. Higher frequency results in more pronounced temperature variations, whereas the presence of nonlocal effects ($\xi = 0.02$) significantly suppresses these fluctuations. This demonstrates that nonlocality stabilizes the thermal field and reduces the intensity of temperature change compared to the local case.

From Fig. 4, mass concentration exhibits a smooth spatial variation along the distance under the action of the inclined force. An increase in frequency ($\omega = 1$) leads to larger fluctuations compared to the lower frequency case ($\omega = 0.5$). The inclusion of nonlocal effects ($\xi = 0.02$) reduces the amplitude of concentration variation and smoothens the profile, indicating a stabilizing influence on mass diffusion.

Fig. 5 shows that the normal stress response varies significantly with distance and exhibits oscillatory behavior due to the inclined force. Higher frequency results in larger stress magnitudes, while the nonlocal parameter ($\xi = 0.02$) lowers the peak values and smoothens the stress curves. This demonstrates that nonlocality mitigates stress concentration and leads to a more uniform stress distribution within the medium.

From Fig. 6, the shear stress varies nonlinearly along the distance and exhibits a clear oscillatory pattern due to the inclined force. Higher frequency ($\omega = 1$) produces significantly

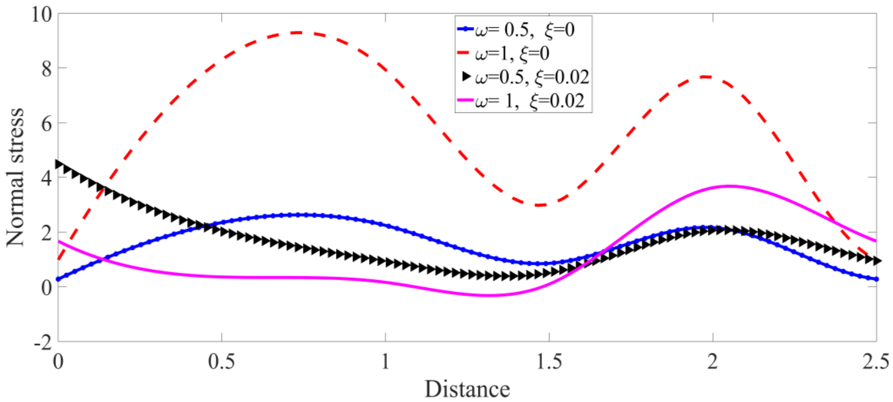

Figure 5. Variation in normal stress with distance *x* due to concentrated force

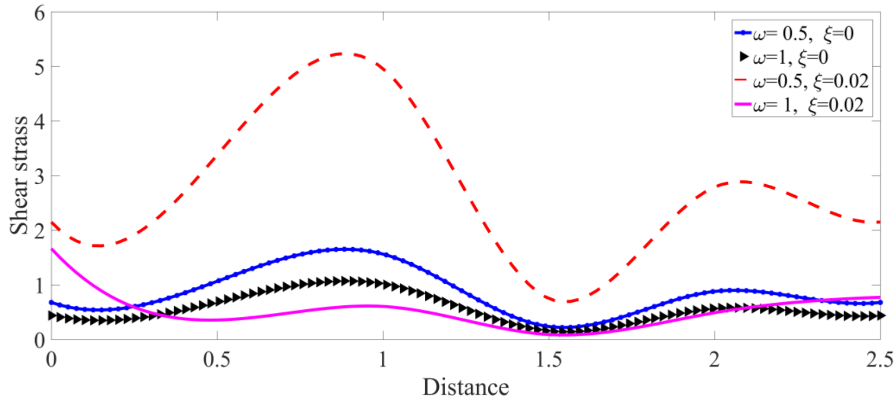

Figure 6. Variation in shear stress with distance *x* due to concentrated force

larger shear stress amplitudes compared to the lower frequency case **(**ω=0.5**)**. The presence of nonlocal effects (ξ = 0.02) reduces the peak shear stress and smoothens the response, indicating a mitigating effect on stress concentration.

The Figs. 7-11 represent the variations of field variables under a uniformly distributed load in a nonlocal solid with distance *x*, where:

I. Red dashed line corresponds to $\omega = 1$ and $\xi = 0$.

II. Blue line with star marker corresponds to $\omega = 0.5$ and $\xi = 0$.

III. Green line corresponds to $\omega = 1$ and $\xi = 0.02$.

IV. Black line with triangle marker (>) corresponds to ω=0.5 and $\xi = 0.02$.

Fig. 7 shows that the vertical displacement exhibits a wave-like variation along the distance due to the inclined force. Higher frequency ($\omega = 1$) results in larger displacement amplitudes, while the lower frequency case ($\omega = 0.5$) exhibits comparatively smaller variations. The inclusion of nonlocal effects ($\xi = 0.02$) significantly reduces the magnitude and smoothens the displacement response.

Fig. 8 shows that the temperature change initially decreases with distance, reaches a minimum around the mid-region, and then increases, indicating thermal wave behavior. Higher frequency produces relatively stronger temperature variations compared to lower frequency. Nonlocal effects

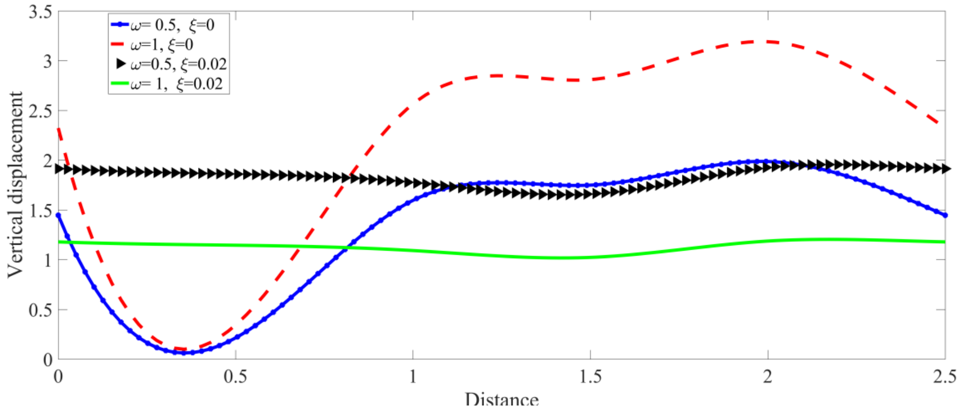

Figure 7. Variation in vertical displacement with distance *x* due to uniformly distributed load

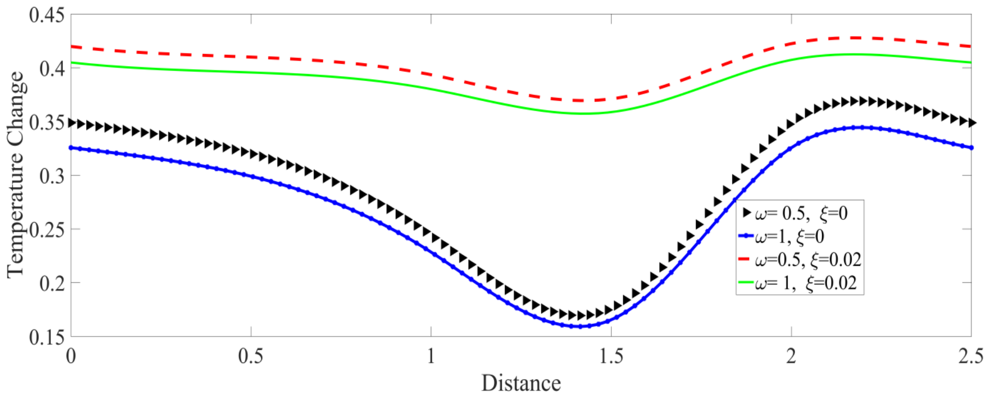

Figure 8. Variation in temperature change with distance *x* due to uniformly distributed load

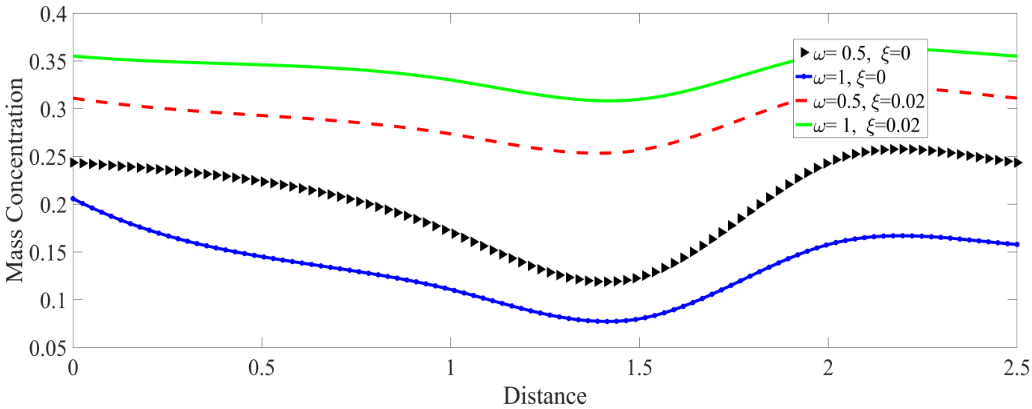

Figure 9. Variation in mass concentration with distance *x* due to uniformly distributed load

$(\xi = 0.02)$ suppress temperature fluctuations and lead to a more uniform and stable thermal distribution.

Fig. 9 shows that the mass concentration decreases gradually with distance, reaches a minimum

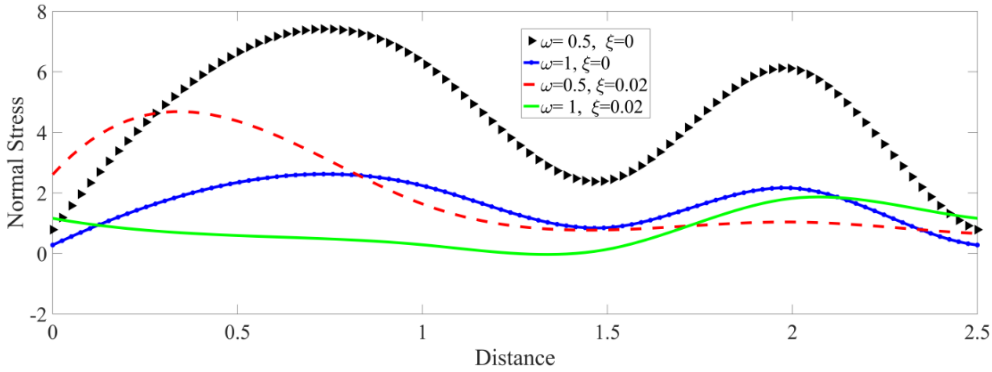

Figure 10. Variation in normal stress with distance *x* due to uniformly distributed load

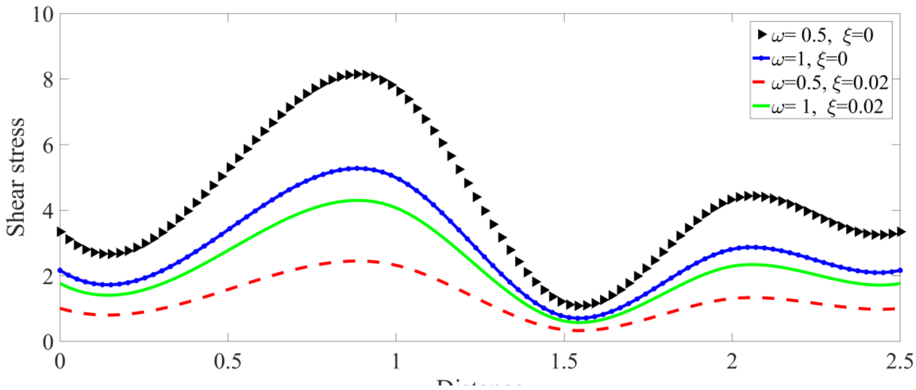

Figure 11. Variation in shear stress with distance *x* due to uniformly distributed load

in the mid-region, and then increases due to the influence of the inclined force. Higher frequency ($\omega = 1$) yields comparatively larger concentration levels than the lower frequency case ($\omega = 0.5$). The presence of nonlocal effects ($\xi = 0.02$) smoothens the concentration profile and reduces the overall variation, indicating stabilized mass diffusion.

Fig. 10 shows that the normal stress varies oscillatory along the distance under the effect of the inclined force. Higher frequency ($\omega = 1$) produces larger stress amplitudes, while the lower frequency case shows comparatively smoother variations. The inclusion of nonlocal effects ($\xi = 0.02$) reduces the peak normal stress and smoothens the stress distribution.

Fig. 11 shows that the shear stress exhibits a wave-like variation with distance due to the inclined force. Increasing the frequency enhances the magnitude of shear stress, whereas nonlocal effects significantly suppress the peak values. This indicates that nonlocality plays an important role in reducing shear stress concentration and stabilizing the mechanical response.

The Figs. 12-16 represent variations in W, T, C, σ_{zz}, and σ_{zx} with distance x due to a linearly distributed load, where:

I. Red dashed line corresponds to $\omega = 1$ and $\xi = 0$.

II. Blue line with star marker corresponds to $\omega = 0.5$ and $\xi = 0$.

III. Green line corresponds to $\omega = 1$ and $\xi = 0.02$.

IV. Black line with triangle marker (>) corresponds to $\omega = 0.5$ and $\xi = 0.02$.

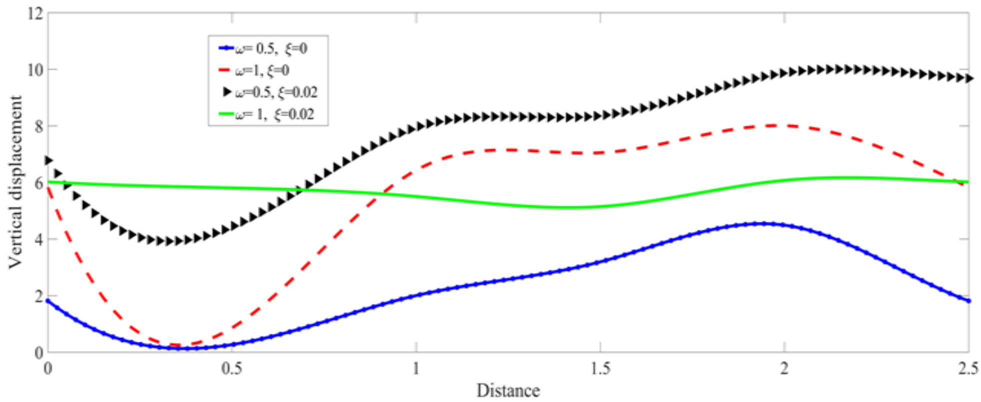

Figure 12. Variation in vertical displacement with distance *x* due to linearly distributed load

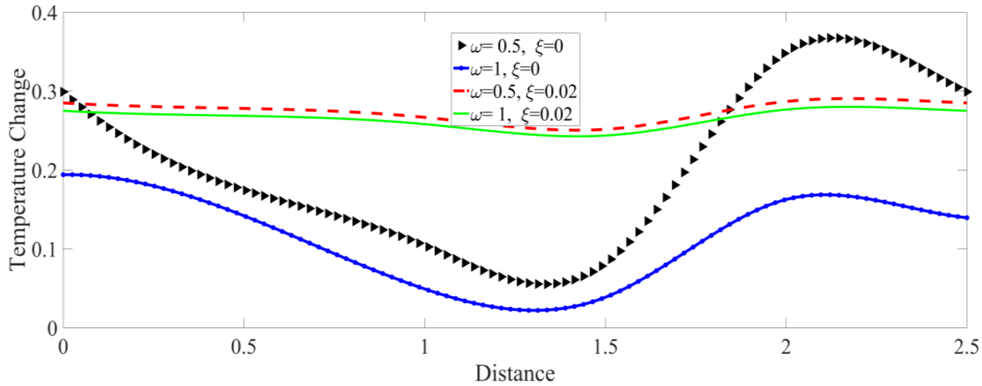

Figure 13. Variation in temperature change with distance *x* due to linearly distributed load

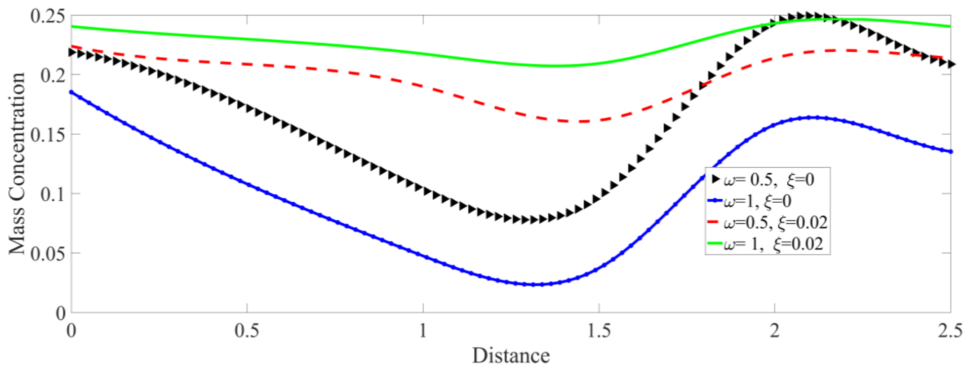

Figure 14. Variation in mass concentration with distance *x* due to linearly distributed load

An applied linearly distributed inclined load on a nonlocal thermoelastic medium produces different response characteristics, as shown in Figs. 12-16.

Fig. 12 shows that the vertical displacement varies nonlinearly with distance and exhibits oscillatory behavior for different angular frequencies (ω) and nonlocal parameters (ξ). Higher angular frequency (ω = 1) results in larger displacement amplitudes compared to the lower

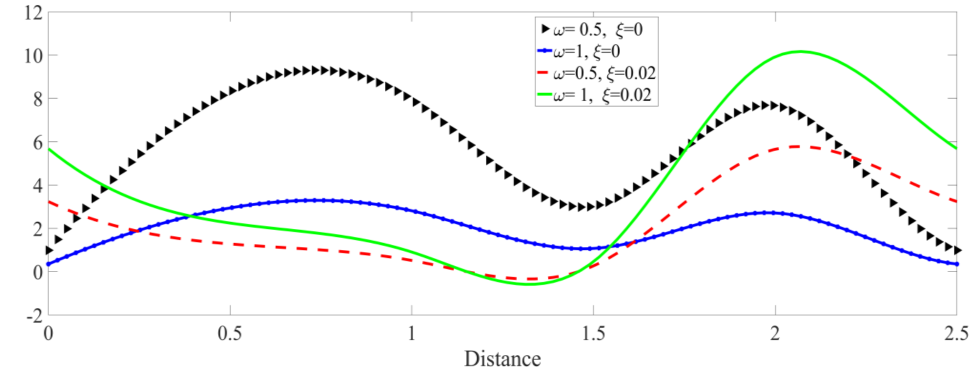

Figure 15. Variation in normal stress with distance *x* due to linearly distributed load

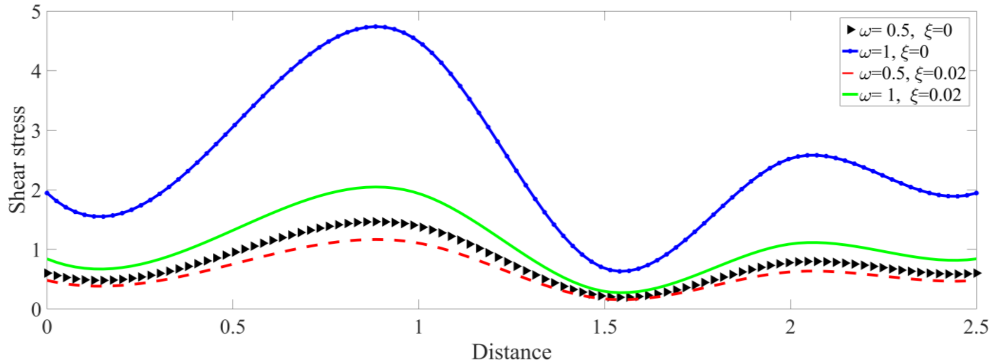

Figure 16. Variation in shear stress with distance *x* due to linearly distributed load

frequency ($\omega = 0.5$). The presence of nonlocal effects ($\xi = 0.02$) smoothens the displacement profile and slightly reduces peak values compared to the local case ($\xi = 0$).

Fig. 13 shows that the temperature change initially decreases with distance, reaches a minimum, and then increases, indicating wave-like thermal behavior. Higher angular frequency produces more pronounced variations in temperature compared to lower frequency. Nonlocal effects ($\xi = 0.02$) reduce thermal gradients and lead to smoother temperature distributions than the classical local model.

Fig. 14 illustrates the variation of mass concentration with distance under an inclined force with a linearly distributed load. The mass concentration initially decreases, attains a minimum near the mid-region, and then increases, indicating non-uniform diffusion behavior. An increase in angular frequency (ω) amplifies the variation, while the nonlocal parameter (ξ) smoothens the response and reduces extreme values compared to the local case ($\xi = 0$).

Fig. 15 depicts the variation of normal stress with distance under an inclined force. The normal stress exhibits oscillatory behavior along the distance, with higher angular frequency (ω) producing larger stress amplitudes. The inclusion of the nonlocal parameter (ξ) smoothens the stress distribution and reduces peak magnitudes compared to the local case ($\xi = 0$). Fig. 16 illustrates the variation of shear stress with distance due to an inclined force. The shear stress shows pronounced fluctuations, and increasing angular frequen**cy** (ω) significantly enhances the stress response. Nonlocal effects ($\xi = 0.02$) lead to a smoother shear stress profile and attenuate extreme values relative to the classical local model.

10. Conclusions

This study investigated the dynamic response of a nonlocal thermoelastic diffusive solid subjected to an inclined load in the frequency domain. The primary objective was to examine the combined influence of nonlocal effects and excitation frequency on the coupled mechanical, thermal, and diffusive fields. The novelty of the work lies in the simultaneous incorporation of nonlocal elasticity and mass diffusion under inclined loading conditions within a frequency-domain framework, providing a more realistic description of size-dependent phenomena than classical local theories.The numerical results reveal that the inclined force generates oscillatory variations in displacement, temperature, mass concentration, and stress distributions throughout the medium. It is observed that increasing the excitation frequency amplifies the mechanical and thermal responses, resulting in higher stress levels and deformation amplitudes. In contrast, the nonlocal parameter exerts a significant stabilizing influence by reducing peak values and smoothing the spatial distributions of all field variables. Physically, the nonlocal parameter accounts for long-range interatomic interactions and introduces a characteristic internal length scale, thereby capturing size-dependent effects that become important in micro- and nano-scale structures.The results demonstrate that the combined effects of frequency and nonlocality play a crucial role in controlling wave propagation, thermal behavior, diffusion characteristics, and stress distribution within the medium. Therefore, neglecting nonlocal effects may lead to inaccurate predictions of the thermoelastic diffusive response in small-scale structures.

The proposed model contributes to the theoretical understanding of coupled thermoelastic diffusion phenomena and may be useful in the design and analysis of advanced composite materials, MEMS/NEMS devices, nano-engineered structures, functionally graded materials, semiconductor components, and aerospace systems. Future studies may extend the present formulation to anisotropic materials, fractional thermoelastic models, rotating media, magneto-thermoelastic interactions, and transient loading conditions.

References

1. Eringen, A.C. (1972). Linear theory of nonlocal elasticity and dispersion of plane waves. International Journal of Engineering Science, 10(5), 425-435. https://doi.org/10.1016/0020-7225(72)90050-X.
2. Eringen, A.C. (1974). Theory of nonlocal thermoelasticity. International Journal of Engineering Science, 12(12), 1063-1077. https://doi.org/10.1016/0020-7225(74)90033-0.
3. Nowacki, W. (1974). The linear theory of micropolar elasticity. Micropolar elasticity, Springer.
4. Ram, P., Sharma, N., Kumar, R. (2008). Thermomechanical response of generalized thermoelastic diffusion with one relaxation time due to time harmonic sources. International Journal of Thermal Sciences, 47(3), 315-323. https://doi.org/10.1016/j.ijthermalsci.2007.02.001.
5. Sharma, N., Kumar, R., Lata, P. (2015). Disturbance due to inclined load in transversely isotropic thermoelastic medium with two temperatures and without energy dissipation. Material Physics and Mechanics, 22(2), 107-117.
6. Srinivasa, A.R., Reddy, J.N. (2017). An overview of theories of continuum mechanics with nonlocal elastic response and a general framework for conservative and dissipative systems. Applied Mechanics Reviews, 69(3), 030802. https://doi.org/10.1115/1.4036723.

7. Kumar, R., Shaloo, D. (2019). Deformation of modified couple stress thermoelastic diffusion in a thick circular plate due to heat sources. CMST, 25(4), 167-176. https://doi.org/10.12921/cmst.2018.0000034.
8. Zenkour, A.M. (2020). Thermoelastic diffusion problem for a half-space due to a refined dual phase-lag Green-Naghdi model. Journal of Ocean Engineering and Science, 5(3), 214-222. https://doi.org/10.1016/j.joes.2019.12.001.
9. Lata, P., Singh, S. (2020). Effects of nonlocality and two temperature in a nonlocal thermoelastic solid due to ramp type heat source. Arab Journal of Basic and Applied Sciences, 27(1), 358-364. https://doi.org/10.1080/25765299.2020.1825157.
10. Abbas, I., Saeed, T., Alhothuali, M. (2021). Hyperbolic two-temperature photo-thermal interaction in a semiconductor medium with a cylindrical cavity. Silicon, 13, 1871-1878. https://doi.org/10.1007/s12633-020-00570-7.
11. Marin, M., Hobiny, A., Abbas, I. (2021). Finite element analysis of nonlinear bioheat model in skin tissue due to external thermal sources. Mathematics, 9(13), 1459. https://doi.org/10.3390/math9131459.
12. Abbas, I., Hobiny, A., Vlase, S., Marin, M. (2022). Generalized thermoelastic interaction in a half-space under a nonlocal thermoelastic model. Mathematics, 10(13), 2168. https://doi.org/10.1080/15397734.2020.1749068.
13. Lata, P., Singh, S. (2022). Axisymmetric deformations in a nonlocal isotropic thermoelastic solid with two temperature. Forces in Mechanics, 6, 100068. https://doi.org/10.1016/j.finmec.2021.100068.
14. Sadeghi, M., Kiani, Y. (2022). Generalized magneto-thermoelasticity of a layer based on the Lord-Shulman and Green-Lindsay theories. Journal of Thermal Stresses, 45(4), 319-340. https://doi.org/10.1080/01495739.2022.2038740.
15. Saeed, T., Abbas, I. (2022). Finite element analyses of nonlinear DPL bioheat model in spherical tissues using experimental data. Mechanics Based Design of Structures and Machines, 50(4), 1287-1297. https://doi.org/10.1080/15397734.2020.1749068.
16. Malik, S., Gupta, D., Kumar, K., Sharma, R., Jain, P. (2023). Reflection and transmission of plane waves in nonlocal generalized thermoelastic solid with diffusion. Mechanics of Solids, 58(1), 161-188. https://doi.org/10.3103/S002565442260088X.
17. Singh, S., Lata, P. (2023). Effect of two temperature and nonlocality in an isotropic thermoelastic thick circular plate without energy dissipation. Partial Differential Equations in Applied Mathematics, 7, 100512. https://doi.org/10.1016/j.padiff.2023.100512.
18. Abbas, I.A., Abdalla, A., Anwar, F., Sapoor, H. (2023). The effects of thermal relaxation times in living tissues under the TPL bio-heat model with experimental study. Advances in Materials Research, 12(1), 31-42. ***https://doi.org/10.12989/amr.2023.12.1.031***.
19. De, A., Purkait, P., Das, P., Kanoria, M. (2023). Effect of magnetic field and inclined load on a two-dimensional thermoelastic medium under gravity. Journal of Multiscale Modelling, 14(3), 2350007. https://doi.org/10.1142/S1756973723500075.
20. Atta, D., Abouelregal, A.E., Sedighi, H.M., Alharb, R.A. (2024). Thermodiffusion interactions in a homogeneous spherical shell based on the modified Moore-Gibson-Thompson theory with two time delays. Mechanics of Time-Dependent Materials, 28(2), 617-638. https://doi.org/10.1007/s11043-023-09598-9.
21. Marin, M., Carrera, E., Abouelregal, A.E. (2024). Structural stability study for porous Cosserat media. Mechanics of Advanced Materials and Structures, 31(15), 3324-3332. https://doi.org/10.1080/15376494.2023.2172239.
22. Abouelregal, A.E., Alhassan, Y., Alsaeed, S.S., Elzayady, M.E., Sedighi, H.M., Kordi, M. (2025). Fractional MGT model for photothermal analysis in rotating semiconductors: Insights into anomalous diffusion and thermal wave propagation. Applied Physics A, 131(6), 1-24. https://doi.org/10.1007/s00339-025-08614-8.
23. Chandel, N., Khalsa, L., Varghese, V. (2025). Non-simple thermoelastic diffusion interaction in a half-space with nonlocality and memory effect. Journal of Thermal Stresses, 1-27. https://doi.org/10.1080/01495739.2024.2449067.
24. Lata, P., Heena. (2025). Frequency-domain analysis of transversely isotropic thermoelastic diffusive

solid with two-temperature. Advances in Materials Research, 14(5), 429-441. https://doi.org/10.12989/amr.2025.14.5.429.

25. Abdul Gaffar, S., Prasad, V.R., Reddy, E.K., Beg, O.A. (2017). Thermal radiation and heat generation/absorption effects on viscoelastic double-diffusive convection from an isothermal sphere in porous media. Journal of the Brazilian Society of Mechanical Sciences and Engineering, 39, 2045-2063. https://doi.org/10.1007/s40430-016-0615-8.
26. Lata, P. (2022). Inclined load effect in an orthotropic magneto-thermoelastic solid with fractional order heat transfer. Structural Engineering and Mechanics, 81(5), 529-537. https://doi.org/10.12989/sem.2022.81.5.529.
27. Gerba, B.F., Lata, P., Singh, S.B. (2025). Dynamic analysis of nonlocal thermoelastic diffusive solids under ramp-type thermal sources. Geomechanics and Engineering, 42(6), 475-487. https://doi.org/10.12989/gae.2025.42.6.475.
28. Bhatti, M.M., Oztop, H.F., Ellahi, R., Duraihem, F.Z. (2026). Numerical analysis of Maxwell fluid flow with quadratic convection under inclined magnetic field employing lie symmetry and Chebyshev spectral techniques. International Journal of Numerical Methods for Heat & Fluid Flow, 36(2), 1140-1169. https://doi.org/10.1108/HFF-09-2025-0682.
29. Ramadan, S.F., Bhatti, M.M., Mekheimer, K.S., Moawad, A.M.A.S., Khalique, C.M. (2026). Magneto-bioconvectiondynamicsofsynovialnanofluids: consequencesofporosity, rheology, and heat generation. Journal of Computational Applied Mechanics, 57(1), 122-133. https://doi.org/10.22059/jcamech.2025.406289.1690.
30. Eringen, A.C. (2002). A continuum theory of superconductivity. Zeitschrift für Angewandte Mathematik und Physik, 53, 1026-1037. ***https://doi.org/10.1007/PL00013844***.
31. Abbas, I., Hobiny, A., El-Bary, A. (2024). The effects of fractional time derivatives in bioheat conduction technique on Tumor thermal therapy. Journal of Non-Equilibrium Thermodynamics, 49(1), 61-72. https://doi.org/10.1063/1.1722351.